YMTHE, Volume *28*

Supplemental Information

COVID-19-Induced ARDS Is Associated with Decreased Frequency of Activated Memory/Effector T Cells Expressing CD11a^{++}

Moritz Anft, Krystallenia Paniskaki, Arturo Blazquez-Navarro, Adrian Doevelaar, Felix S. Seibert, Bodo Hölzer, Sarah Skrzypczyk, Eva Kohut, Julia Kurek, Jan Zapka, Patrizia Wehler, Sviatlana Kaliszczyk, Sharon Bajda, Constantin J. Thieme, Toralf Roch, Margarethe Justine Konik, Marc Moritz Berger, Thorsten Brenner, Uwe Kölsch, Toni L. Meister, Stephanie Pfaender, Eike Steinmann, Clemens Tempfer, Carsten Watzl, Sebastian Dolff, Ulf Dittmer, Mohamed Abou-El-Enein, Timm H. Westhoff, Oliver Witzke, Ulrik Stervbo, and Nina Babel

Supplemental Appendix

Table of Contents

Supplement tables

Table S1. Clinical characteristics of the study patients according to disease severity

	Disease Severity		P value
	COVID-19 Control	ARDS	
Number of Patients	35 (77.8%)	10 (22.2%)	-
Chest CT abnormalities			
Bilateral ground-glass opacity	28 (80.0%)	10 (100.0%)	0.320
Pleural effusion	2 (5.7%)	1 (10.0%)	0.539
Median laboratory findings			
pO2/FiO2 mmHg	NA	129 [86-166.75]	-
Platelets (cells/nL)	179 [160.5-266.5]	189.5 [149.25-249.5]	0.827
Hemoglobin (g/dL)	12.7 [11.9-14.25]	8.85 [8.425-9.2]	<0.001
C-reactive protein (mg/dL)	8.9 [4.65-13.75]	15.4 [11-27]	0.015
Procalcitonin (ng/mL)	0.065 [0.02-0.265]	2.425 [1.405-3.37]	<0.001
Lactate dehydrogenase (U/L)	305 [272.5-396]	469.5 [357-584]	0.013
Total bilirubin (mg/dL)	0.6 [0.3-0.9]	1.5 [1.1-2.675]	<0.001
GFR (mL/min/1.73m^2)	46 [41.975-53.5]	45.9 [39-50]	0.935
Therapy			
Oxygen	19 (54.3%)	10 (100.0%)	0.008
Intravenous antibiotics	26 (74.3%)	10 (100.0%)	0.173
Admission to intensive care unit	0 (0.0%)	10 (100.0%)	<0.001
Mechanical Ventilation	0 (0.0%)	10 (100.0%)	<0.001
Hydrocortisone	1 (2.9%)	1 (10.0%)	0.399
Hydroxychloroquine	1 (2.9%)	6 (60.0%)	<0.001
Aciclovir	0 (0.0%)	1 (10.0%)	0.222
Outcome			
Length of hospitalization (days)	11 [7-26.5]	39 [34.75-43.5]	0.016
Currently hospitalized	4 (11.4.0%)	0 (0.0%)	1.000
Death	0 (0.0%)	6 (60.0%)	<0.001
Discharge	31 (88.6%)	4 (40.0%)	0.004

Quantitative variables are expressed as median [IQR] and compared by the Kruskal-Wallis test. Categorical variables are compared employing Fisher's exact test. GFR estimated by MDRD. NA: indicate not applicable

Table S2. Association of sex with the potential markers of COVID-19 severity

Cell population	P value sex	P value ARDS
Lymphocytes (cells/nL)	0.188	0.038
$CD3^+$ (cells/nL)	0.173	0.066
NK cells (cells/nL)	0.866	0.044
Eosinophil cells	0.230	0.017
% CM among $CD4^+$	0.072	0.004
% $CD4^+HLA\text{-}DR^+$ among $CD4^+$	0.724	0.036
% $CD8^+HLA\text{-}DR^+$ among $CD8^+$	0.582	0.010
% $CD4^+CD11a^{++}$ among $CD4^+$	0.010	0.074
% $CD8^+CD11a^{++}$ among $CD8^+$	0.094	<0.001
% $CD4^+CD28^+$ among $CD4^+$	0.167	<0.001
% Transitional among $CD19^+$	0.497	0.197
% Anti-S $CD4^+CD154^+$	0.691	0.040
% Anti-S $CD8^+CD137^+$	0.985	0.058
% Anti-S $CD8^+CD137^+IFN\gamma^+$	0.882	0.049
% Anti-S $CD4^+CD154^+IL\text{-}2^+$	0.601	0.066
% Anti-S $CD8^+CD137^+IL\text{-}2^+$	0.835	0.059
% Anti-S $CD8^+CD137^+TNF\alpha^+$	0.188	0.038

Association of sex with potential markers of COVID-19 severity at the initial visit was assessed by bivariate regression.

Table S3. Frequency of patients with detectable antigen specific T cell subpopulations

			Disease Severity		
T cell subpopulation	Visit	All patients	COVID-19 Control	ARDS	P value
$CD4^+CD154^+$	Initial	18 (66.7%)	10 (58.8%)	8 (80.0%)	0.406
	Follow-up	16 (100.0%)	12 (100.0%)	4 (100.0%)	-
$CD4^+CD154^+GrB^+$	Initial	11 (40.7%)	8 (47.1%)	3 (30.0%)	0.448
	Follow-up	5 (31.2%)	4 (33.3%)	1 (25.0%)	1.000
$CD4^+CD154^+IFN\gamma^+$	Initial	18 (66.7%)	11 (64.7%)	7 (70.0%)	1.000
	Follow-up	13 (81.2%)	9 (75.0%)	4 (100.0%)	0.529
$CD4^+CD154^+IL2^+$	Initial	19 (70.4%)	10 (58.8%)	9 (90.0%)	0.190
	Follow-up	14 (87.5%)	10 (83.3%)	4 (100.0%)	1.000
$CD4^+CD154^+TNF\alpha^+$	Initial	18 (66.7%)	10 (58.8%)	8 (80.0%)	0.406
	Follow-up	14 (87.5%)	10 (83.3%)	4 (100.0%)	1.000
$CD8^+CD137^+$	Initial	15 (55.6%)	7 (41.2%)	8 (80.0%)	0.107
	Follow-up	9 (56.2%)	5 (41.7%)	4 (100.0%)	0.088
$CD8^+CD137^+GrB^+$	Initial	15 (55.6%)	8 (47.1%)	7 (70.0%)	0.424
	Follow-up	8 (50.0%)	5 (41.7%)	3 (75.0%)	0.569
$CD8^+CD137^+IFN\gamma^+$	Initial	10 (37.0%)	4 (23.5%)	6 (60.0%)	0.101
	Follow-up	8 (50.0%)	4 (33.3%)	4 (100.0%)	0.077
$CD8^+CD137^+IL2^+$	Initial	8 (29.6%)	2 (11.8%)	6 (60.0%)	0.025
	Follow-up	5 (31.2%)	2 (16.7%)	3 (75.0%)	0.063
$CD8^+CD137^+TNF\alpha^+$	Initial	8 (29.6%)	3 (17.6%)	5 (50.0%)	0.102
	Follow-up	3 (18.8%)	2 (16.7%)	1 (25.0%)	1.000

The presence of SARS-CoV-2-reactive T cells was evaluated in 27 patients at the initial visit (17 COVID-19 Control and 10 ARDS) and 16 at follow-up (12 COVID-19 Control and 4 ARDS). Differences between patient groups for initial and follow-up for each T-cell subpopulation are calculated by Fisher's exact test.

Table S4. Frequency of patients with detectable polyfunctional SARS-CoV-2 reactive T cells

	Number of expressed cytokines	Initial		P value	Follow-Up		P value
		COVID-19 Control	ARDS		COVID-19 Control	ARDS	
$CD4^+$ T cells	1	94.1% (16/17)	100% (10/10)	1.000	100% (17/17)	100% (4/4)	1.000
	2	70.6% (12/17)	100% (10/10)	0.124	82.4% (14/17)	100% (4/4)	1.000
	3	52.9% (9/17)	50% (5/10)	1.000	52.9% (9/17)	100% (4/4)	0.131
	4	29.4% (5/17)	10% (1/10)	0.355	23.5% (4/17)	25% (1/4)	1.000
$CD8^+$ T cells	1	100% (17/17)	100% (10/10)	1.000	76.5% (13/17)	100% (4/4)	0.546
	2	70.6% (12/17)	90% (9/10)	0.363	70.6% (12/17)	100% (4/4)	0.532
	3	23.5% (4/17)	50% (5/10)	0.219	23.5% (4/17)	75% (3/4)	0.088
	4	0% (0/17)	10% (1/10)	0.393	17.6% (3/17)	25% (1/4)	1.000

Percentage (number) of patients with detectable polyfunctional SARS-CoV-2-reactive T cells. Differences between patient groups for initial and follow-up are calculated by Fisher's exact test.

Supplement figures

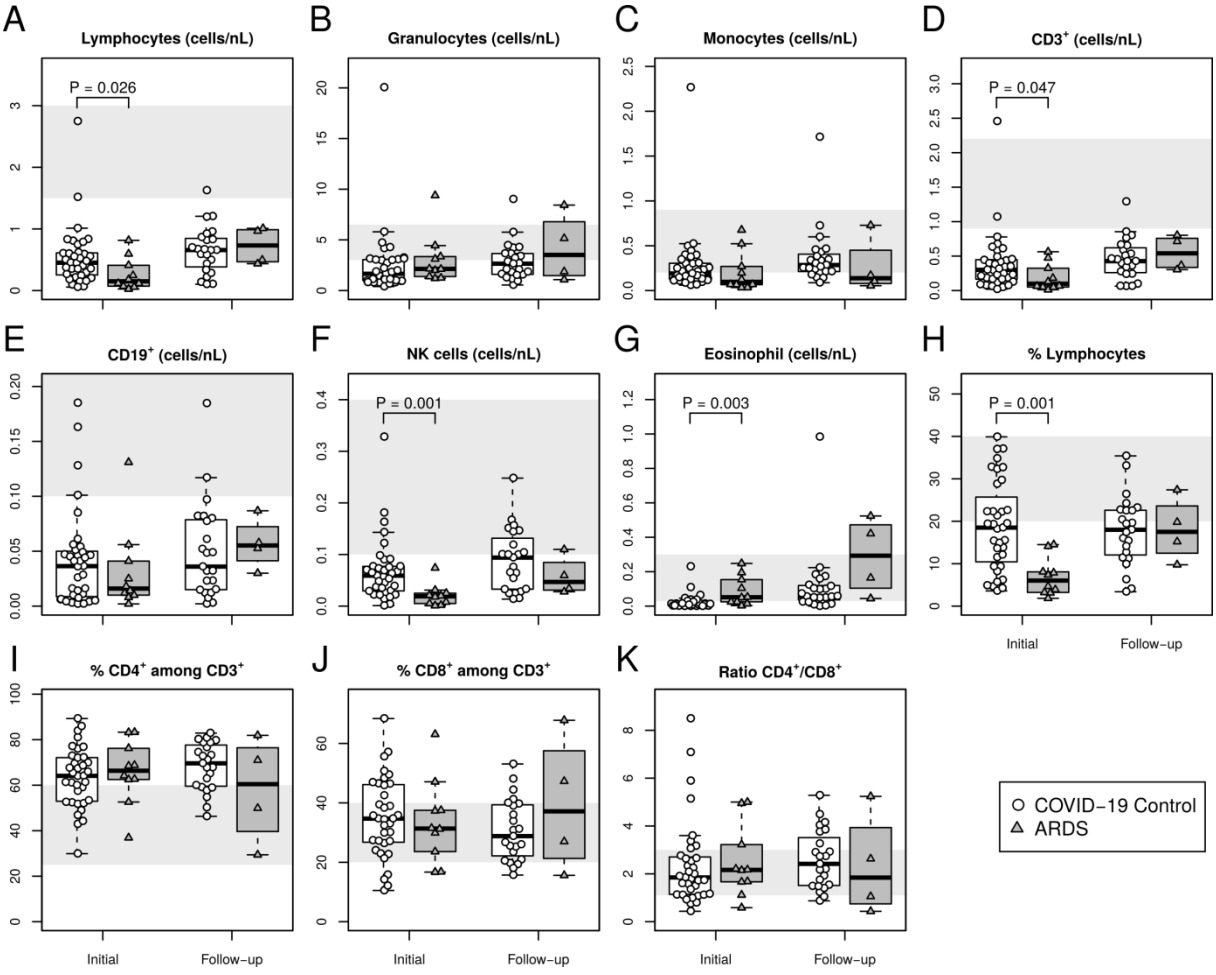

Figure S1. ARDS is associated with severe lymphopenia.

Circulating immune cell subsets were characterized in patients confirmed COVID-19 at the initial visit using multiparametric flow cytometry. In total, 45 patients from the COVID-19 Control (n=35, in white) or ARDS (n=10, in gray) sub-cohorts were analyzed at the initial visit and at follow-up. In all cases, the left boxplots show the data for the initial visit, while the right boxplots depict the data at follow-up. Immune cell subsets in peripheral blood were evaluated according to the gating strategy in Fig. S8. Cell counts were evaluated for (A) Lymphocytes, defined as $CD45^{+}SSC^{low}$, (B) Granulocytes, defined as $CD45^{+}SSC^{high}$, and (C) Monocytes, defined as $CD45^{+}SSC^{intermediate}$. Within the lymphocytes the cell counts were assessed for (D) T cells, defined as $CD3^{+}$ lymphocytes, (E) B cells, defined as $CD19^{+}CD3^{-}$, (F) natural killer cells (NK), defined as $CD56^{+}CD3^{-}$. (G) The cell counts of the Granulocyte subpopulation Eosinophils, defined as $CD45^{+}SSC^{high}CD16^{-}$. The frequency of (H) lymphocytes in whole blood, (I) T helper cells, defined as $CD3^{+}CD4^{+}CD8^{-}$ and (J) cytotoxic T cells identified as $CD3^{+}CD8^{+}CD4^{-}$ among $CD3^{+}$ T cells. (K) Ratio of $CD4^{+}$ and $CD8^{+}$ T cells in I and J. The shaded area indicates the reference range in healthy individuals.

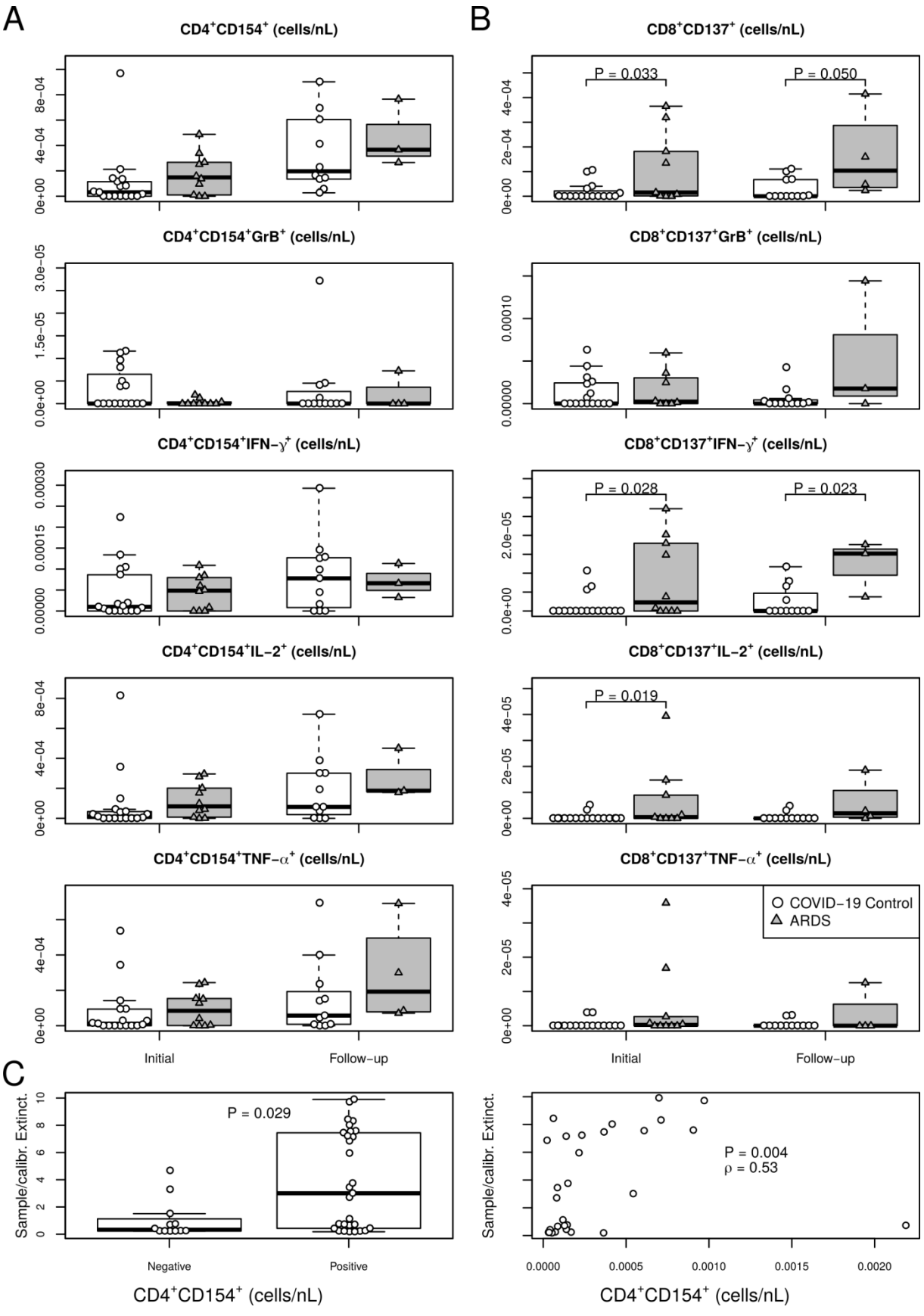

Figure S2 Increased number and functional activity of SARS-CoV-2-reactive T cells in ARDS patients.

The presence and functional status of SARS-CoV-2-reactive T cells was evaluated using PBMCs, isolated from the peripheral blood of 27 patients (17 COVID-19 Control, in white, and 10 ARDS, in gray). Defrosted PBMCs rested for 24 hours before treatment with overlapping peptide pools covering the SARS-CoV-2 S-protein. The cells were stimulated for a total of 16 hours and in the presence of Brefeldin A for the last 14 hours. The complete gating strategy is presented in Fig. S7. (A) $CD4^+CD154^+$ counts (first row) for ARDS and COVID-19 Control patients at the initial visit (left boxplots) and follow-up (right boxplots), and counts of $CD4^+CD154^+$ cells expressing granzyme B (GrB), INF-γ, IL-2, and TNF-α (row two to four). (B) $CD8^+CD137^+$ counts (first row) for ARDS and COVID-19 Control patients at the initial visit (left boxplots) and follow-up (right boxplots), and counts of $CD8^+CD137^+$ cells expressing granzyme B (GrB), INF-γ, IL-2, and TNF-α among (row two to four). (C) Comparison of the relative titers of SARS-CoV-2 S-protein specific IgG antibodies, measured by ELISA and evaluated as ratio to an internal control for samples with detectable SARS-CoV-2 specific $CD4^+$ T cells (left) and cellcorrelation of the relative titers of SARS-CoV-2 with the counts of SARS-CoV-2 specific $CD4^+$ T cells (right) cell. Note that no measurements of IgG antibodies were available for ARDS patients.

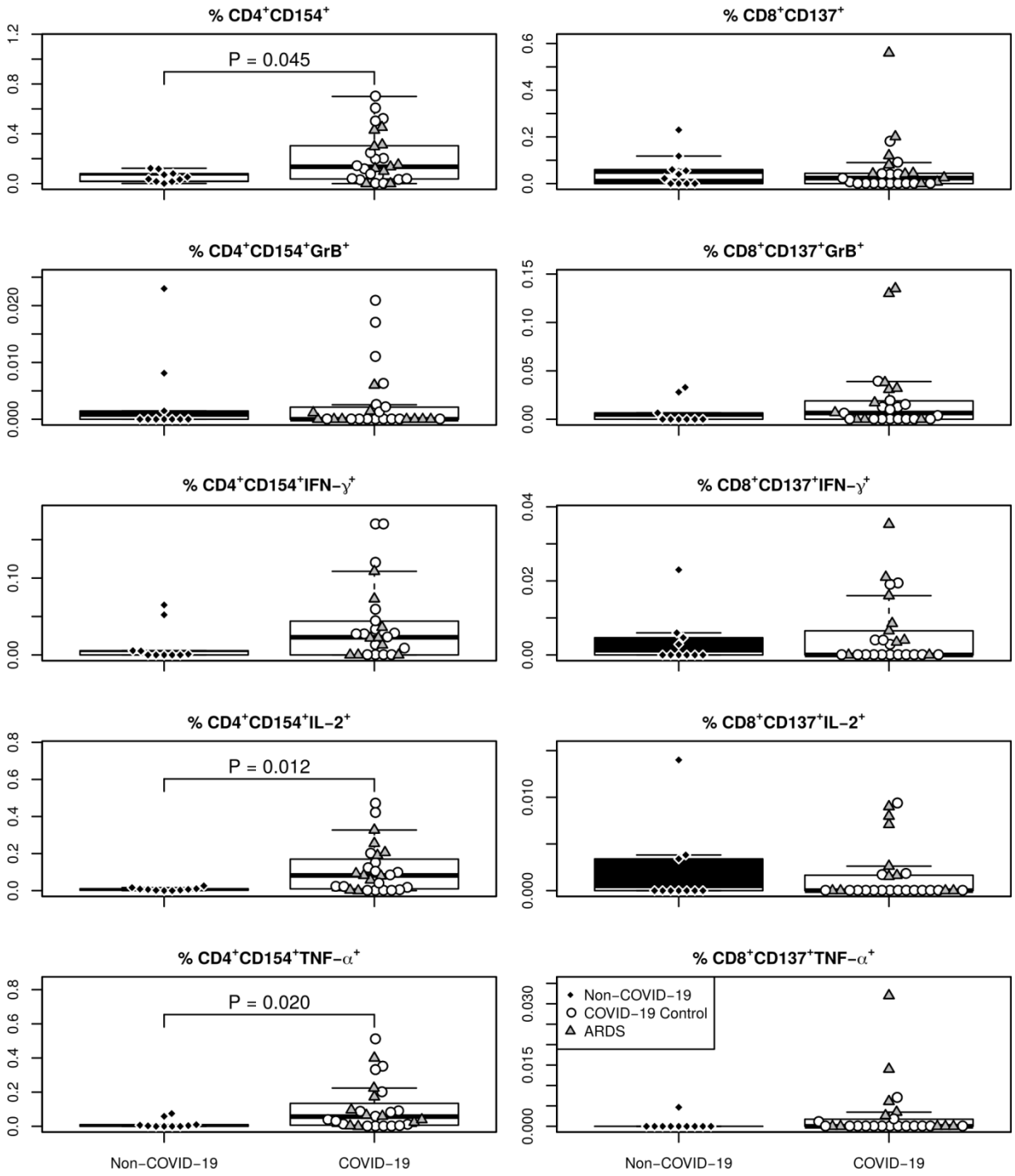

Figure S3. Increased frequency and functional activity of SARS-CoV-2-reactive T cells in COVID-19 patients compared to COVID-19 unexposed healthy blood donors.

The presence and functional status of SARS-CoV-2-reactive T cells was evaluated in COVID-19 unexposed healthy donors in comparison to the cohort of COVID-19 patients. For the unexposed patients, blood samples were collected before pandemics onset and stored at -80°C. For COVID-19 cohort, the last available sample per patient was included in the analysis. The complete gating strategy is presented in Fig. S6.

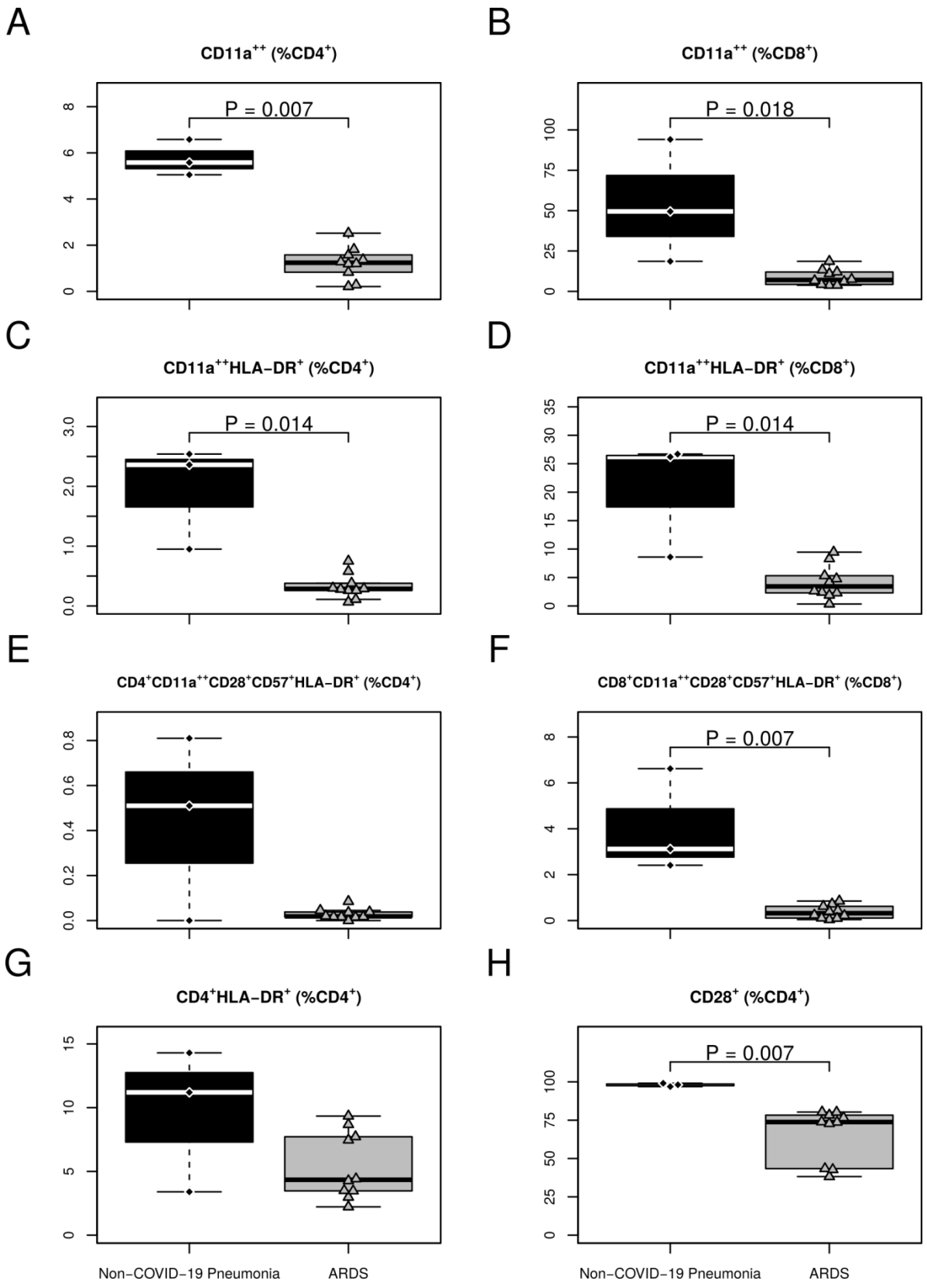

Figure S4. The observed alterations of T cell subsets for ARDS patients were COVID-specific

Potential markers of COVID-19 severity were analyzed for their specificity. Peripheral blood from patients with COVID-19-associated ARDS (ARDS, n=10, in gray) and patients with non-COVID-19 pneumonia and sepsis on mechanical ventilation (Non-COVID-19 Pneumonia, n=3, in gray) at the initial visit was subjected to evaluation for differentiation and activation state of T- cell using multiparametric flow cytometry. The subsets of the $CD3^+$ T cells were identified according to the gating strategy in Fig. S9 and S10. (A-B) The frequency of $CD11a^{++}$ cells among $CD4^+$ (A) and $CD8^+$ (B) $CD3^+$ T cells. (C-D) The frequency of $CD11a^{++}HLA\text{-}DR^+$ expressing cells among $CD4^+$ (C) and $CD8^+$ (D) $CD3^+$ T cells. (E-F) The frequency of $CD11a^{++}HLA\text{-}DR^+CD28^+CD57^+$ expressing cells among $CD4^+$ (E) and $CD8^+$ (F) $CD3^+$ T cells. (G) Expression of HLA-DR among and $CD4^+$ T cells. (H) Expression of CD28 among $CD4^+$ T cells.

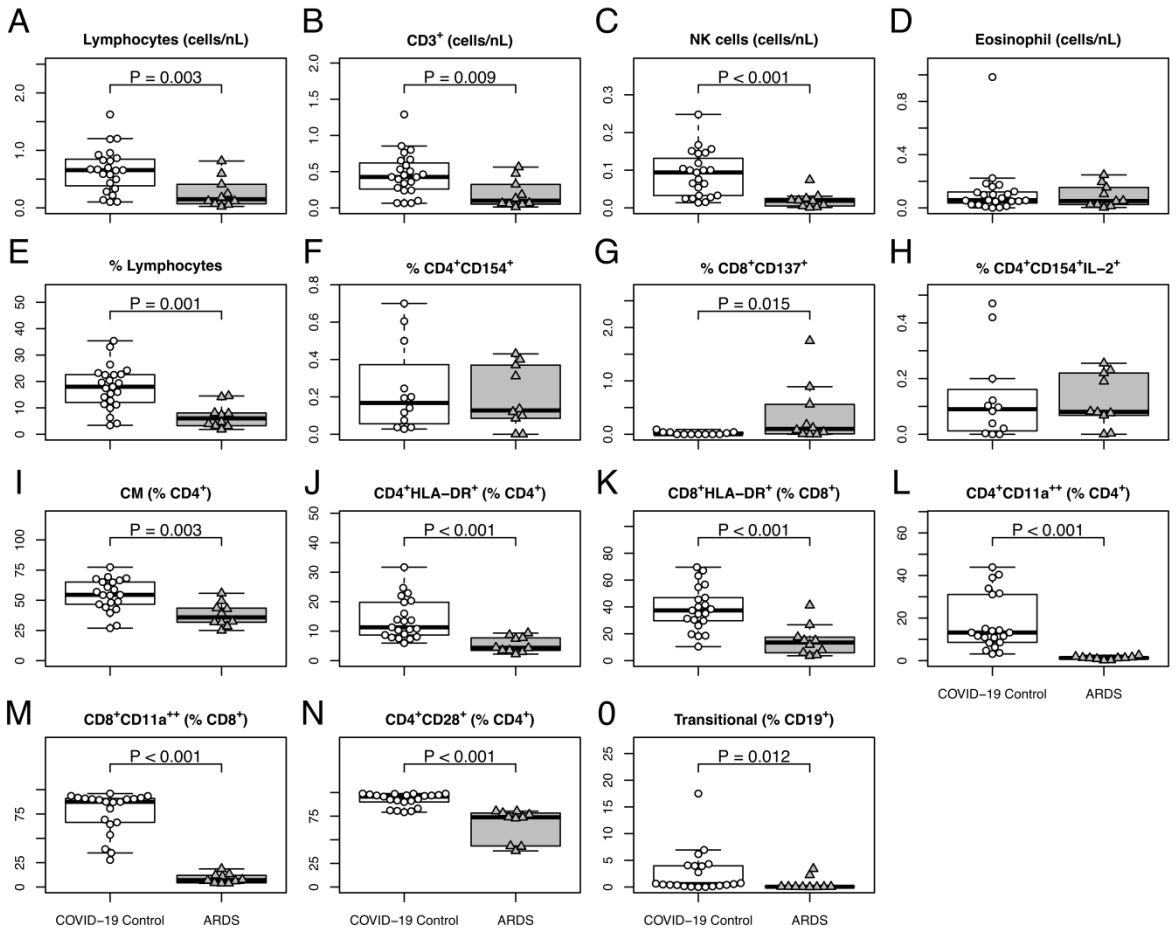

Figure S5. The observed immunological alterations for ARDS patients were not due to the differences in sampling time

To demonstrate that the observed results are not due to the differences in sampling time, we additionally performed analyses using samples of both groups obtained at similar time points in days after initial diagnosis (7 [3-10] for COVID-19 control vs. 8 [6-15] days in ARDS cohort; P=0.766). The comparison was performed for all markers that showed a significant effect of ARDS at the initial visit (Figures S1, 2 and 3). ARDS patients (n=10, in gray) were compared with the COVID-19 Control patients (n=23, in white). The subsets were identified according to the gating strategies in Fig. S6-10. (A-D) The counts of lymphocytes, $CD3^+$ cells, NK cells and eosinophils and (E) the frequency of lymphocytes. (F-H) Frequency of SARS-CoV-2-reactive $CD4^+CD154^+$, $CD8^+CD137^+$ cells and IL-2-secreting $CD4^+CD154^+$ cells. (I-O) Frequency of CM $CD4^+$, $CD4^+$HLA-DR^+, $CD8^+$HLA-DR^+, $CD4^+CD11a^{++}$, $CD8^+CD11a^{++}$, $CD4^+CD28^+$ and transitional B cells.

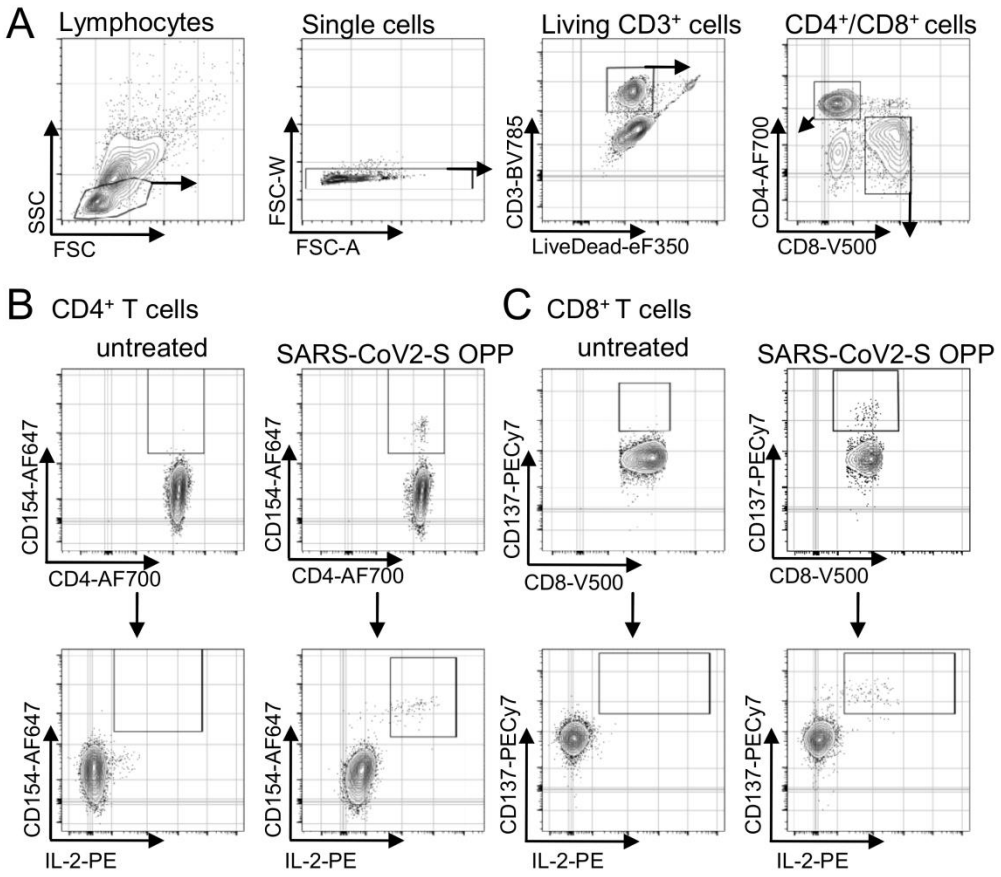

Figure S6. Gating strategy for detection of cytokine producing $CD4^+$ and $CD8^+$ antigen specific T cells.

Isolated PBMCs were stimulated with SARS-CoV-2 spike protein OPPs or left untreated for 16h. (A) Lymphocytes were gated based on side and forward scatter profile, doublets were excluded and living T cells were identified as $CD3^+$ and Live/Dead-Marker negative cells, expressing either CD4 or CD8. Antigen specific T cells were identified as $CD4^+CD154^+CD137^+$ T-helper cells (B) or $CD8^+CD137^+$ cytotoxic T cells (C). Within the antigen specific T cells, intracellular staining of cytokines and granzyme B was used to identify effector cells.

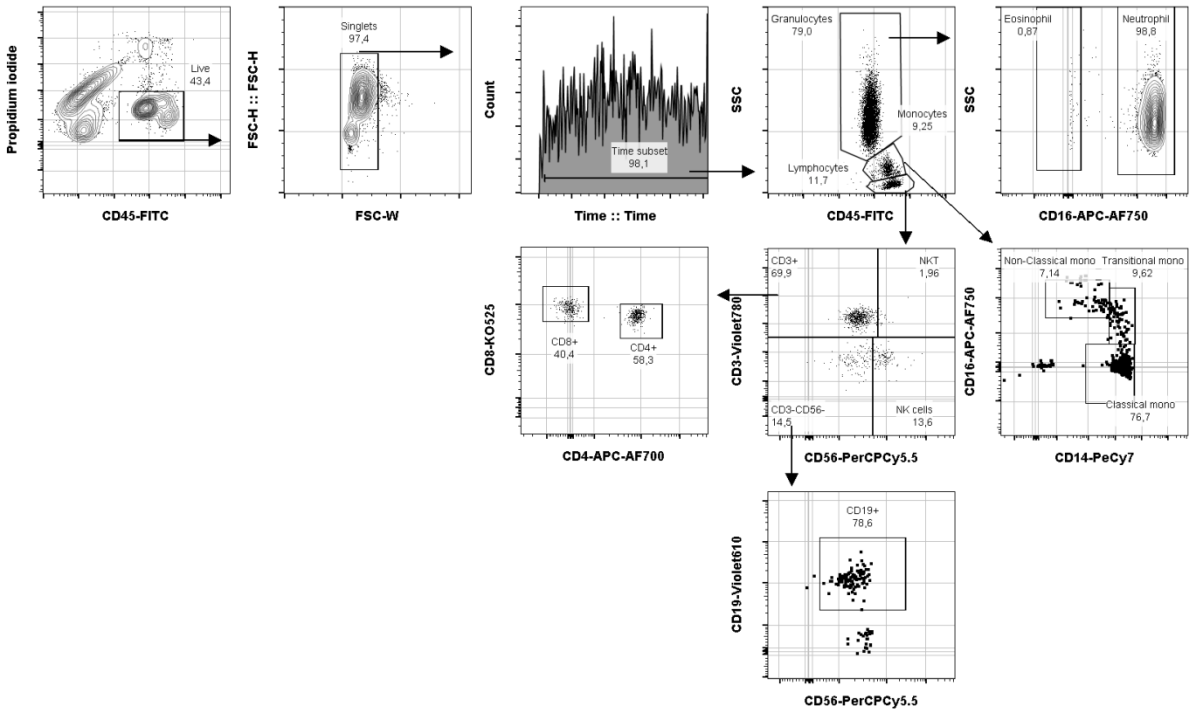

Figure S7. Gating strategy for identification of main immune cell populations.

Whole blood was diluted 1:1 in staining solution prior to erythrocytes lysis. Live cells were identified as negative for propidium iodide and doublets were excluded. Granulocytes, monocytes and lymphocytes were distinguished by CD45 and side scatter profile. Granulocytes were separated by CD16 in Eosinophiles ($CD16^{-}$) and Neutrophiles ($CD16^{+}$). Monocytes were divided by the expression of CD14 and CD16 into classical- ($CD14^{++}CD16^{-}$), intermediate- ($CD14^{++}CD16^{+}$) and non-classical Monocytes ($CD14^{+}CD16^{+}$). Lymphocytes were separated by CD3 and CD56 in NK ($CD3^{-}CD56^{+}$), NKT ($CD3^{+}CD56^{+}$) and T cells ($CD3^{+}CD56^{-}$) and T cells were further distinguished into $CD4^{+}$ helper T cells and $CD8^{+}$ cytotoxic T cells. B cells were identified as CD3/CD56 double negative and CD19 positive cells.

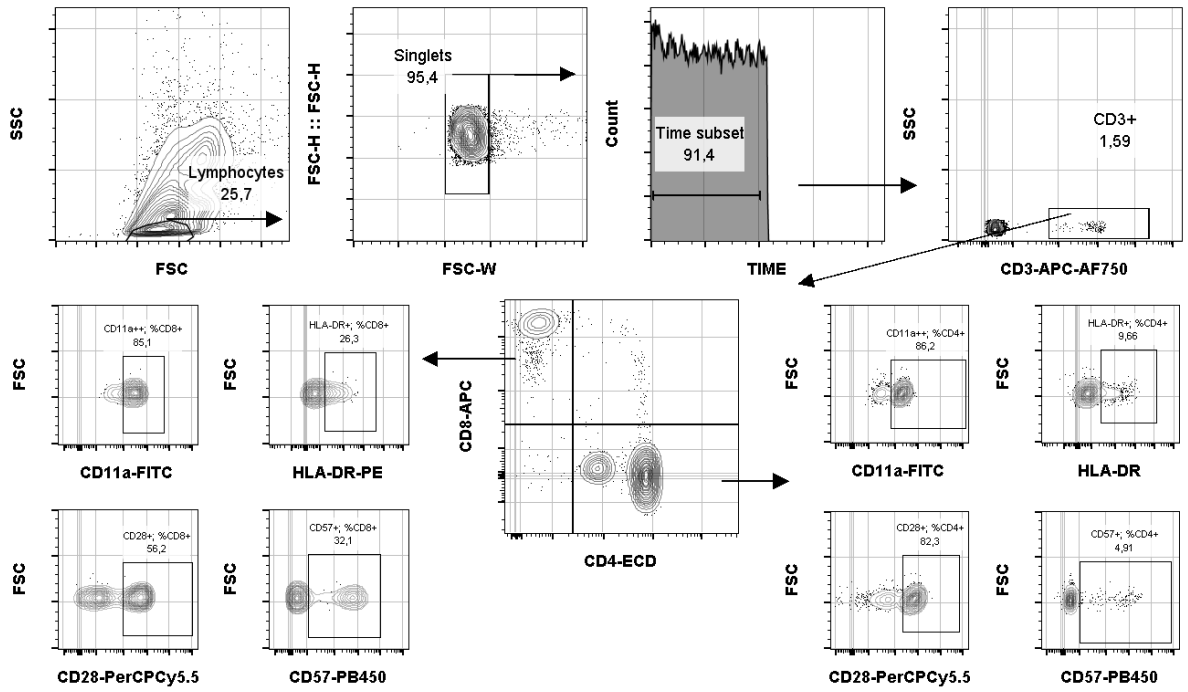

Figure S8. Gating strategy for identification of activated T cells.

Whole blood was diluted 1:1 in staining solution prior to erythrocytes lysis. Living lymphocytes were identified by their forward and sideward scatter profile and doublets were excluded. T cells were identified as $CD3^+$ and separated by expression of CD4 and/or CD8 into double negative ($CD4^-CD8^-$), double positive ($CD4^+CD8^+$), T-helper cells ($CD4^+CD8^-$) and cytotoxic T cells ($CD4^-CD8^+$). The expression of activation marker CD11a, HLA-DR, CD28 and CD57 was assessed on $CD4^+$ and $CD8^+$ single positive T cells.

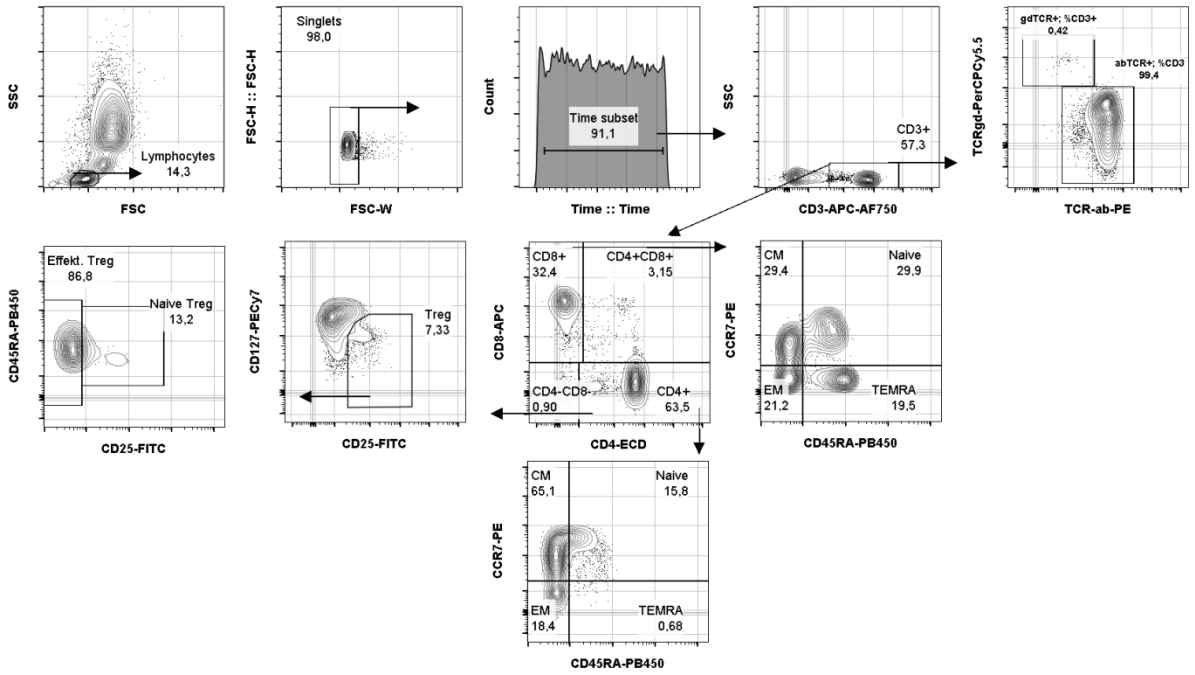

Figure S9. Gating strategy for identification of memory and regulatory T cells.

Whole blood was diluted 1:1 in staining solution prior to erythrocytes lysis. Living lymphocytes were identified by their forward and sideward scatter profile and doublets were excluded. T cells were identified by the expression of CD3 and separated into αβ-T cells and γδ-T cells by staining with TCR antibodies against TCRαβ and TCRγδ antibodies. Additionally, $CD3^+$ T cells were divided into T-helper cells ($CD4^+CD8^-$) and cytotoxic T cells ($CD4^-CD8^+$). Both T cell subsets were further divided by the expression of CD45RA and CCR7 into naïve ($CD45RA^+CCR7^+$), central memory (CM, $CD45RA^-CCR7^+$), effector memory (EM, $CD45RA^-CCR7^-$) and T effector RA (TEMRA, $CD45RA^+CCR7^-$) T cells. Additionally, regulatory T cells (Tregs) were identified as $CD4^+CD25^+CD127^+$ and further separated by their expression of CD45RA into Naïve ($CD45RA^+$) and effector Tregs ($CD45RA^-$).

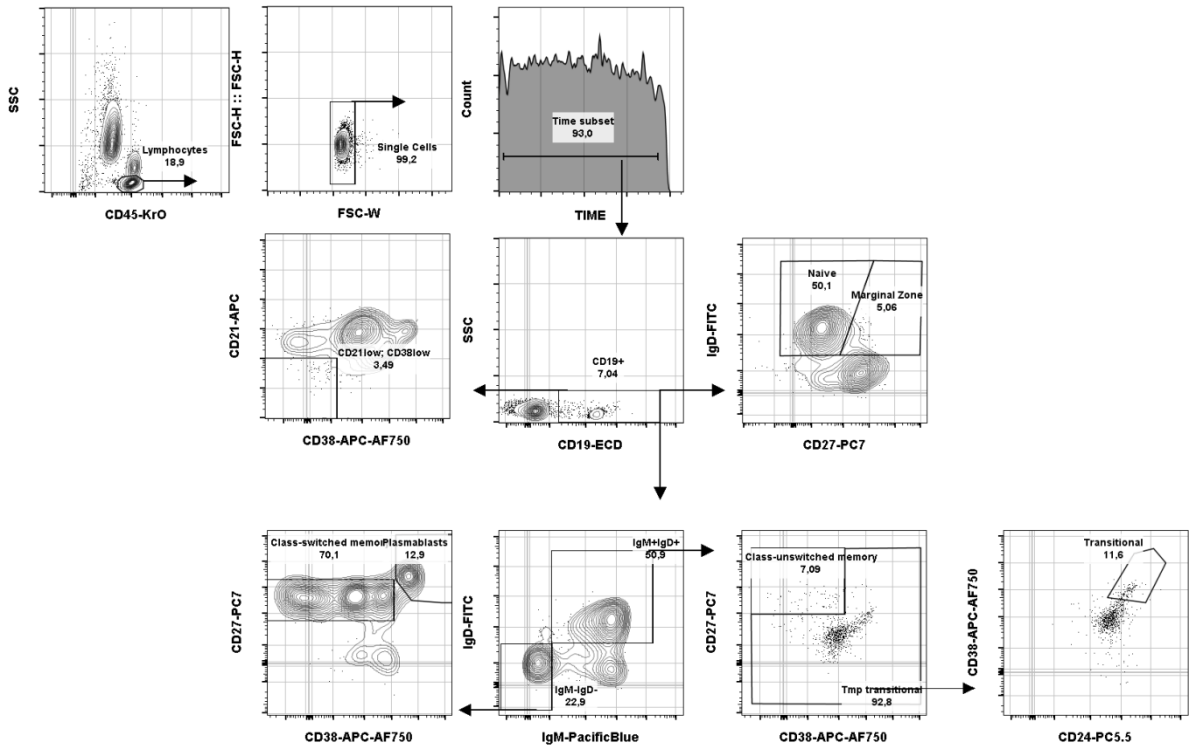

Figure S10. Gating strategy for identification of B cell subpopulations.

Whole blood was diluted 1:1 in staining solution and afterwards erythrocytes were lysed. Living lymphocytes were identified by their forward and sideward scatter profile and doublets were excluded. B cells were identified by the expression of CD19 and separated into naïve ($IgD^{+}CD27^{-}$), marginal zone B cells ($IgD^{+}CD27^{+}$) and $CD21^{low}CD38^{low}$ B cells. Additionally, B cells were separated by expression of IgM and IgD into double negative ($IgM^{-}IgD^{-}$) and double positive ($IgM^{+}IgD^{+}$) cells. Double negative cells could be separated by CD38 and CD27 into class-switch memory B cells and Plasmablasts ($CD27^{high}CD38^{high}$). IgM/IgD double positive B cells were further divided into class-unswitched memory B cells ($CD27^{+}CD38^{-}$) and $CD38^{high}CD24^{high}$ transitional B cells.